Bioorganic & Medicinal Chemistry 17 (2009) 2327–2335

Contents lists available at ScienceDirect

Bioorganic & Medicinal Chemistry

journal homepage: www.elsevier.com/locate/bmc

Design and synthesis of 4-methoxyphenylacetic acid esters as 15-lipoxygenase inhibitors and SAR comparative studies of them

Hamid Sadeghian [a,*], Neda Attaran [b], Zeinab Jafari [b], Mohammad Reza Saberi [c,†], Mehdi Pordel [a], Mohammad Mahdi Riazi [b]

[a] Department of Laboratory Sciences, School of Paramedical Sciences, Mashhad University of Medical Sciences, Mashhad 91389-13131, Iran
[b] Department of Chemistry, Faculty of Sciences, Ferdowsi University of Mashhad, Mashhad 91775-1436, Iran
[c] School of Pharmacy, Pharmaceutical Research Center, Mashhad University of Medical Sciences, BuAli Square, Mashhad 9196773117, Iran

ARTICLE INFO

Article history:
Received 30 August 2008
Revised 18 January 2009
Accepted 9 February 2009
Available online 13 February 2009

Keywords:
Methylenation
SLO
Protein modeling
Docking
15-HLO

ABSTRACT

A group of 4-methoxyphenylacetic acid esters were designed, synthesized and evaluated as potential inhibitors of soybean 15-lipoxygenase (SLO) on the basis of eugenol and esteragol structures. Compounds 7d–**e** showed the best IC_{50} in SLO inhibition (IC_{50} = 3.8 and 1.9 μM, respectively). All compounds were docked in SLO active site and showed that carbonyl group of compounds is oriented toward the Fe^{III}–OH moiety in the active site of enzyme and fixed by hydrogen bonding with hydroxyl group. It is assumed that lipophilic interaction of ligand–enzyme would be in charge of inhibiting the enzyme activity. The selectivity of the synthetic esters in inhibiting of 15-HLOb was also compared with 15-HLOa by molecular modeling and multiple alignment techniques.

1. Introduction

Our interest in 4-methoxyphenylacetic acid derivatives as lipoxygenase inhibitors emerges from the early work by our groups, in which the soybean 15-lipoxygenase inhibition of eugenol and its esters was reported.[1] It is well documented that mammalian lipoxygenases (LO's) are non-heme iron-containing enzymes responsible for the oxidation of polyunsaturated fatty acids and esters to hydroperoxy derivatives.[2] There are heterogeneous family of enzymes distributed widely throughout the plant and animal kingdoms,[3] and named according to the position at which a key substrate, arachidonic acid (AA), is oxidized. Among the mammalian lipoxygenases involved in the etiology of human disease, 5-lipoxygenase (5-LO) is now well established as a target for reducing the production of leukotrienes (important in particular asthma).[4] More recently, 15-lipoxygenase (15-LO) has emerged as an attractive target for therapeutic intervention.[5] 15-LO has been implicated in the progression of certain cancers[6,7] and chronic obstructive pulmonary disease (COPD).[8] Evidence for the inhibition of 15-LO in the treatment of vascular disease is, however, most compelling.[9] Both transgenic and knockout studies implicate a role for 15-LO in atherogenesis.[10,11] The enzyme is abundantly expressed in macrophages residing within the atherosclerotic lesion.[5] In addition, the immediate products of 15-LO oxidation of AA and linoleic acid (LA) have been shown to be pro-inflammatory[12] and pro-thrombotic.[13]

It is also found that 15-LO is linked to cardiovascular complications due to participation in oxidative modification of low-density lipoproteins (LDL), leading to the development of atherosclerosis.[14]

Chanez and colleagues[15] explained that in vivo 15-HLOa (human 15-lipoxygenase) has antitumor effects in human airway carcinomas and promote apoptotic pathway. They believed that neoplastic tissues from human airway carcinomas demonstrated non-specific staining for human 15-HLOa as compared with normal tissues. By contrast, in human prostate tumors 15-HLOa was overexpressed as compared with normal adjacent tissue,[7] and 15-HLOb was poorly expressed in prostate tumors.[16] In PC3 cells, 13(*S*)-HODE, one of the 15-HLOa metabolites, upregulated MAP kinase, whereas in contrast 15(*S*)-HETE, the 15-HLOb metabolite, downregulated MAP kinase.[17] Taken together, these findings including the upregulation of 15-HLOa within the airway tissue of smoking patients with chronic bronchitis, provided new evidence of possible acquired abnormalities linked to airway inflammation. The bronchial epithelium is clearly a key player in inflammation and structural changes in airway diseases. Its rich content in 15-HLOa- and 15-HLOb-derived products highlight their potential as new target for therapeutic interventions.

Three different strategies have been developed to inhibit the LO's pathway.[18] They involve (i) redox inhibitors or antioxidants,

* Corresponding author. Tel.: +98 0511 7610111; fax: +98 0511 7628088.
E-mail address: hd_sn@yahoo.com (H. Sadeghian).
† Tel.: +98 511 7112611/5; fax: +98 511 7112596.

0968-0896/$ - see front matter © 2009 Elsevier Ltd. All rights reserved.
doi:10.1016/j.bmc.2009.02.009

Table 1
Enzyme inhibitory assessment and docking analysis data of consensus conformers for SLO

Compound	IC_{50} (μM)	Compound	IC_{50} (μM)	K_i	E_d (Kcal/mol}	ΔG_b (Kcal/mol)	RMSD
Eugenol	38.2 ± 1.9	**7a**	56.2 ± 1.5	1.13e-4	−6.27	−5.38	24.86
Methyleugenol	96.1 ± 3.3	**7b**	32.0 ± 1.6	5.85e-5	−7.05	−5.77	24.27
Esteragol	64.1 ± 1.5	**7c**	11.6 ± 10.2	3.11e-5	−7.84	−6.15	24.24
1	43 ± 1.4	**7d**	3.8 ± 0.3	1.07e-5	−8.71	−6.78	23.98
2	137 ± 5.5	**7e**	1.9 ± 0.2	5.66e-6	−9.50	−7.16	23.52
3	33 ± 2.1	**7f**	35.0 ± 2.1	6.66e-6	−9.33	−7.06	22.74
4	145 ± 3.9	**7g**	34.4 ± 0.8	5.72e-5	−7.08	−5.79	23.72
8	>200	**7h**	35.7 ± 1.7	2.37e-5	−7.49	−6.31	22.85
		71	88.1 ± 0.6	2.42e-4	−6.15	−4.93	23.47
		7J	38.7 ± 0,9	5.73e-5	−5.84	−5.79	22.93
		7k	56.5 ± 3.4	8.88e-5	−6.44	−5.53	23.36
		71	64.0 ± 1.1	1.43e-4	−5.87	−5.25	23.13

ΔG_b: Estimated free energy of bonding, E_d: final docking energy, K_i: estimated inhibition constant and RMSD: root-mean-square deviation from reference structure. The IC_{50} values are given as mean ± SD.

which interfere with the redox cycle of 15-LO, (ii) iron-chelator agents, and (iii) non-redox competitive inhibitors, which compete with AA to bind the enzyme active site.

In this study, (i) some esters of 4-methoxyphenylacetic acid were designed, synthesized and their activities were identified as the mean of IC_{50} on soybean 15-LO (SLO), then (ii) common bonding model of 4-methoxyphenylacetic acid esters in SLO active site, (iii) SAR study of inhibitors to propose key features of this class of inhibitors, (iv) and theoretical potency of these compounds for inhibiting modeled 15-HLOa and 15-HLOb are reported.

2. Results and discussion

Considering our previous work on eugenol and esters[1] we tested the inhibitory property of eugenol, methyleugenol and esteragol on the SLO (substrate: linoleic acid). The results showed IC_{50} = 38.2 ± 1.9, 96.1 ± 3.3 and 64.1 ± 1.5 μM for the mentioned enzyme, respectively. It is notable that no other products such as hydroperoxy are isolated from action of the LO enzyme on methyleugenol and esteragol as substrate (assuming hydroproxy is supposed to be obtained if the redox pathway is blocked and the inhibitor acts through its allylic group in reaction with the enzyme active site similar to the oxidation of natural unsaturated fatty acids).[‡] Considering the IC_{50} results of the three compounds we decided to study the effect of some changing in esteragol double bond on inhibitory potency of this compound. At first 1-methoxy-4-(2-methylallyl)benzene (**2**) and 1-methoxy-4-(2-ethylallyl)benzene (**4**) were synthesized via methylenation of 1-(4-methoxyphenyl)acetone (**1**) and 1-(4-methoxyphenyl)-2-butanone (**3**). The results of enzyme assay showed low potency of the mentioned allyl compounds for inhibition of lipoxygenase activity (IC_{50} = 137 ± 5.5 and 145 ± 3.9 μM for compounds **2** and **4**, respectively). Fixing of ethyl group of compound **4** in a ring by synthesis of 6-methoxy-2-methylene-1,2,3,4-tetrahydronaphthalene (**6**) from 6-methoxy-2-tetralone (**5**) lead to no inhibitory potency even at 200 μM. It is interesting to see that the precursor compounds **1** and **3** showed better inhibitory activity towards SLO by 43 ± 1.4 and 33 ± 2.1 μM.

Regarding the mechanism of hydroperoxydation and docking procedure in this study, one might conclude that carbonyl moiety of compounds **1** and **3** is able to inhibit lipoxygenase activity through hydrogen bonding interaction with hydroxyl group of iron atom of the enzyme. We followed the study by testing methyl ester of 4-methoxyphenylacetic acid (**7a**) for lipoxygenase inhibitory activity in which the IC_{50} was 56.2 ± 1.5 μM. For investigating of general bonding model of these carbonyl compounds in SLO, a series of aliphatic esters of 4-methoxyphenylacetic acid (**7b–l**) were synthesized and evaluated for lipoxygenase inhibitory activity. The synthetic esters **7a–l** showed a broad range of inhibition activity on the enzyme (IC_{50} = 1.9–88.1 μM; Table 1). Compound **7e** having *n*-pentyl substituent was the most potent inhibitor at 1.9 ± 0.22 while the isobutyl analogs (**7i**) presented lowest activity (IC_{50} = 88.1 ± 0.64 μM).

The esters **7a–l** were docked into the active site of SLO to determine the inhibitory mechanism. The experimental results matched with theoretical K_i of docking study for those models in which carbonyl group oriented toward iron atom similar to orientation of linoleic acid peroxide in the active site. We generated 100 docked conformers of **7a–l** corresponding in ADT software. A detailed inspection of each independent inhibitor conformers revealed that more than 40% of docking results had nearly identical orientations in which carbonyl group of each inhibitor oriented toward Fe core. One conformer from each esters cluster whose carbonyl moiety superposed on linoleic acid peroxy part was adopted as the 'consensus' structure and used for further analysis (Fig. 1) (Scheme 1).[1,19]

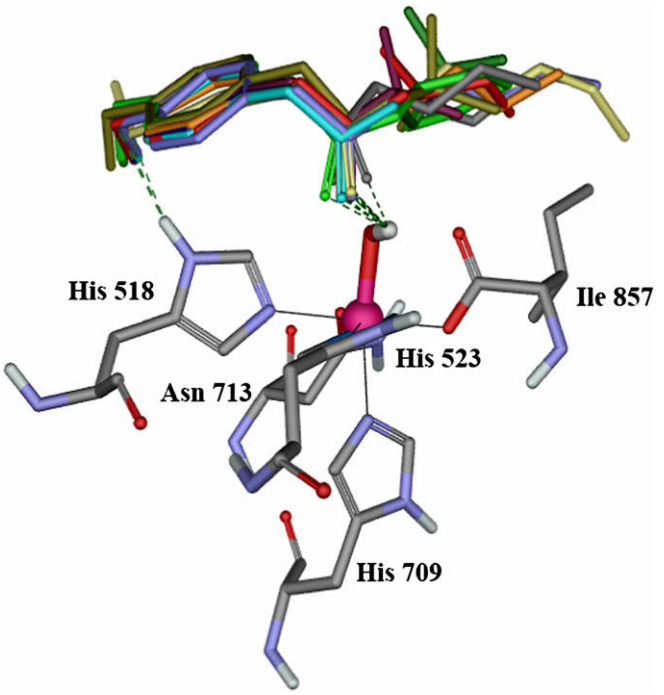

Figure 1. Consensus bonding conformations of compounds **7a–l** in the SLO active site (color sticks). Hydrogen bonds are shown by dashed green lines and the Fe atom bond to hydroxyl group, distinguished by purple color.

[‡] Substrate (100 μM) was reacted with soybean LO enzyme (167 U/mL) in 3 mL borate buffer solution (0.1 M, pH 9) at 20 °C for 15 min. The mixture was then analyzed by UV at 230–270 nm and no absorption of vinyl benzene formation was appeared over the blank solution.

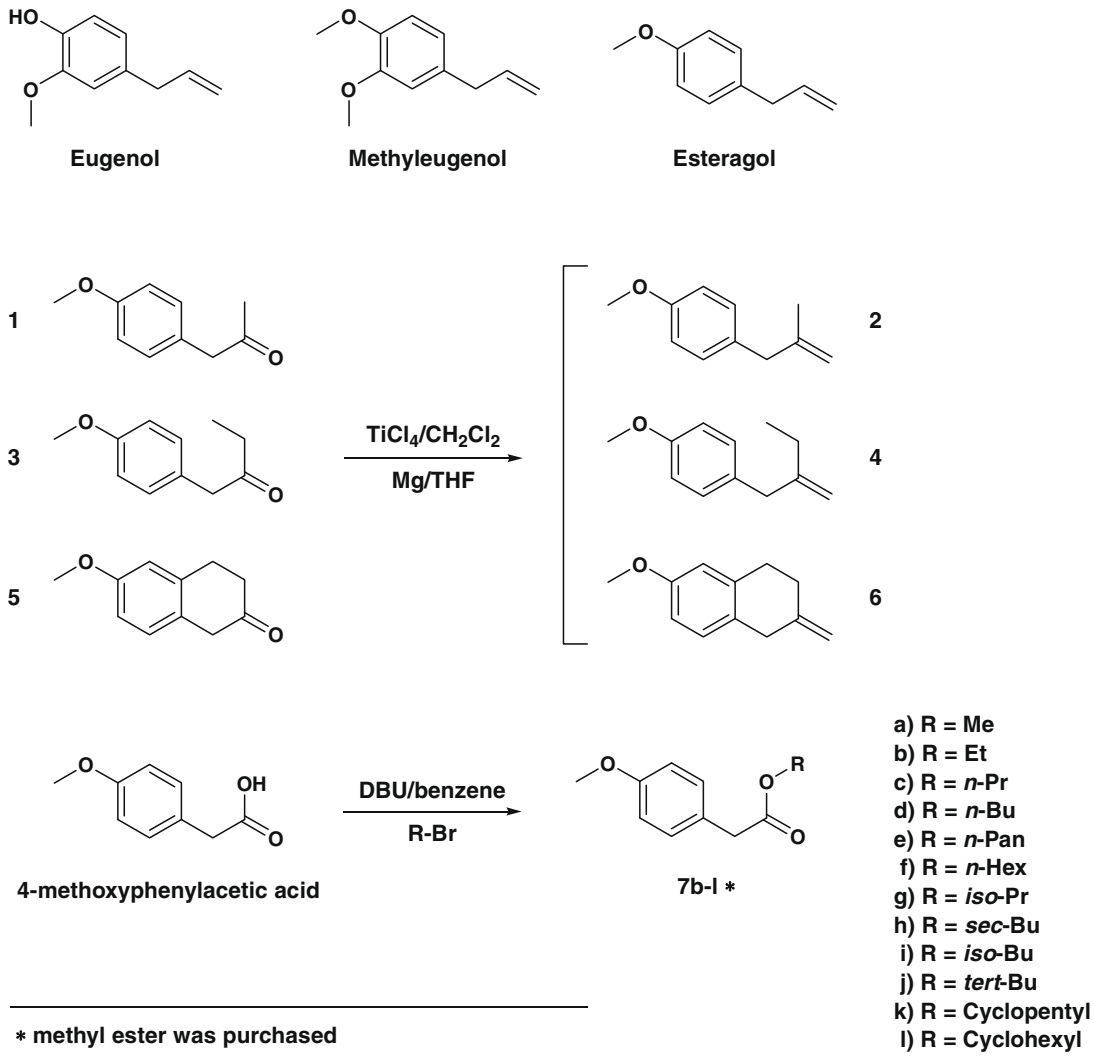

Scheme 1. Molecular structures of eugenol, methyleugenol and esteragol. General procedures for the synthesis of compounds **2**, **4**, **6** and **7b–l**.

It seems that the alkyl part of the esters has hydrophobic interaction with the cavity formed by side chain of Leu^{273}, Thr^{274}, Leu^{277}, Ile^{557}, Leu^{560}, Ile^{772}, Leu^{773} and Ile^{857} (pocket A) while benzyl core has the same interaction with Leu^{515}, Trp^{519}, Leu^{565}, Val^{566} and Ile^{572} side chains (pocket B) (Fig. 2). Ile^{857} is one of the high conserved residues directly bond to the iron atom. The most critical residues, that is, Ile^{557}, Leu^{565}, Leu^{773} and Ile^{572} appeared close to the active site (Fig. 2). X-ray presentation of LA into SLO[20] presents lipophil interaction of the side chain of Ile^{857} with C-16–C-18 of LA. It also indicates that Ile^{557}, Leu^{565} and Leu^{773} lay within 4–6 Å of Fe^{3+}–OH and both leucines are near the reactive site, C-11–C-13, of LA (C-11: hydrogen abstraction site, C-13: oxygenation site). Although Ile^{572} is far from Fe^{3+}–OH, (at 9 Å) but still forms part of the substrate-bonding cavity. Each of these residues provides a large surface to interact with natural substrate, particularly Leu^{565} and Leu^{773}. Mutating of the Ile or Leu to an Ala opens up space within the bonding pocket of SLO, leading to altered $H^{\cdot}$ transfer kinetics.[21] The Ile^{557}→Ala and Ile^{572}→Phe mutants decreased k_{cat} by 2 folds from WT (wild type), While Leu^{565}→Ala and Leu^{773}→Ala decreased k_{cat} by 60 and 1000-folds, respectively, indicating that these hydrophobic residues (specially Leu^{565} and Leu^{773}) contribute significantly to catalysis.[21] According to the result of multiple alignment, six amino acids Ile^{557}, Leu^{565}, Ile^{572}, Val^{566}, Leu^{773} and Ile^{857} are found to be conserved over all species (Fig. 3). We can also view in Figure 1 that the proposed orientation of docked molecules has hydrogen bond with conserved His^{518} and hydroxyl of iron complex via 4-methoxy and carbonyl group, respectively.

The K_i of consensus structure of the esters have good non-linear relationship with IC_{50} results except for **7f** and **7h** (Fig. 4). This relation comes from tendency of the alkyl moiety for filling the empty lipophilic space of Thr^{274}, Leu^{277}, Ile^{557}, Leu^{560}, Leu^{773} and Ile^{857} side chains (Fig. 2). The exception of **7f** and its high increase in IC_{50} value versus **7e** imply that the lipophilic cavity of pocket A has a restricted tunnel about 6 Å from oxygenation site of LA. If the consensus structure of the esters are compared with X-ray presentation of LA into SLO, most conformity between *n*-pentyl ester (**7e**) and LA can be determined. The docking calculation suggests that **7f** would be fairly active. It is notable that the docking performed on PDB format of X-ray presentation of LA into SLO with no flexibility of residues in the active site pocket. So it can open a space as large as *n*-hexyl portion for suitable occupation and finally results the best K_i. But in real condition (Section 4) the mentioned space seems to be smaller which can lead to decrease in IC_{50} result and finally causes the observed disconformity between modeling prediction and biological data.

There are significant differences in size, sequence, and substrate preference between the plant and animal LOs, but the overall fold

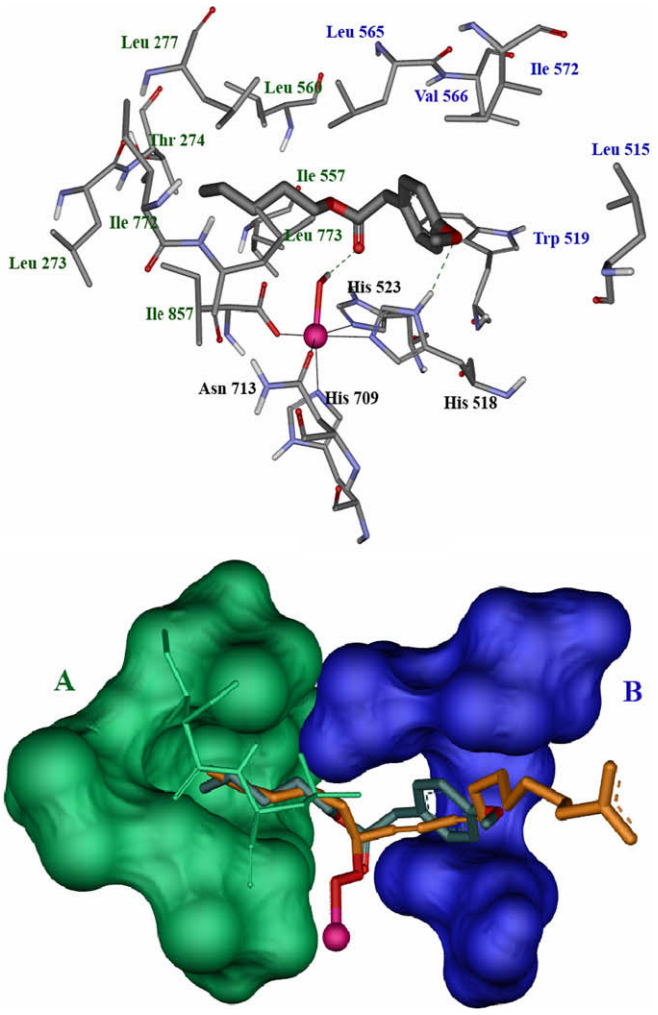

Figure 2. Above: stick view of the consensus bonding conformations of ester **7e** which has lipophilic interaction with amino acids of two pockets A (green symbols) and B (blue symbols). Below: solvent surface view of pockets A (except for Ile^{772} and Leu^{773}) and B with 13(*S*)-proxy-9(*Z*)-2,11(*E*)-octadecadienoic acid (light brown stick) and **7e** (atom colored stick).

and geometry of the non-heme iron-binding site are conserved.[22] The structures of SLO and modeled 15-HLOa and 15-HLOb demonstrate a high level of conservation within 14 Å (around the LA into SLO X-ray view) in the active site pocket. Thus the structures of both 15-HLO could be superposed on the SLO with RMS for the C-α atoms of around 1.16–1.24 Å in the mentioned region (Fig. 5). The largest differences between the SLO and both 15-HLO active site pockets were found in residues of initial part of α2 helix (Fig. 5). In SLO, α2 helix consists of 18 residues (Leu^{273}–Ala^{291}) while the 15-HLOa and 15-HLOb include 16 (Glu^{176}–Leu^{192}) and 18 residues (Glu^{120}–Gln^{128}), respectively (Table 2).

In the active site pocket of the superposed SLO and both 15-HLO, the C-α of amino acids laying within 7 Å of the LA are well fitted except for Leu^{273}, Thr^{274} and Leu^{277} of SLO in contrast with Ile^{173} and Asp^{174} of 15-HLOa (Fig. 6). Free space of catalytic region around the pocket B seems to be larger for SLO and 15-HLOb in comparison with 15-HLOa (Fig. 6). This lacking comes from steric occupation of aromatic side chains of Phe^{353} and Phe^{552} in the 15-HLOa cavity. The data of Table 2 show that the pocket A of SLO and 15-HLOb is more lipophile than its equal in 15-HLOa. This is because of Arg^{403} and Gln^{596} in 15-HLOa in contrast with Leu^{560} and Ile^{772} in SLO and Leu^{415} and Leu^{609} in 15-HLOb. The similarity between residues of SLO pocket A and the superposed in 15-HLOb, from point of view of C-α situational conformity and lipophilicity, could be an evidence for selectivity of the large and lipophile esters toward type b mammalian 15-LO in comparison with type a. To prove this hypothesis the inhibitory potency of compounds **7b** and **7e**, as small and large compound, was determined against 15-lipoxygensae a and b (human recombinant). It was interesting to see IC_{50} values of 56.7 ± 1.4 and 63.2 ± 2.1 μM for compound **7e** and 30.9 ± 1.3 and 11.7 ± 0.8 μM for compound **7e** against 15-HLOa and 15-HLOb, respectively. These results confirm that the large and lipophil ester **7e** is selective toward 15-HLOb by ~three-fold and it cannot be seen for the small analog such as **7b**.

In summary the present study introduces that long chain and lipophile 4-methoxyphenylacetic acid esters such as **7e** behave as the best SLO inhibitors (IC_{50} = 1.9 μM) and also as a selective inhibitor of 15-HLOb when compared with 15-HLOa. The importance of these compounds could be more highlighted when we consider their easy synthesis pathway and high yield.

3. Materials and methods

3.1. Chemistry

The methylenation of some carbonyl compounds using Mg–$TiCl_4$ in THF/CH_2Cl_2 was reported in last literatures.[23] This Mg–$TiCl_4$-promoted CH_2-transfer reaction of CH_2Cl_2 represents an extremely simple, practical, and efficient methylenation of a variety of ketones and aldehydes, especially in enolizable or sterically hindered ketones. Methylenation of compounds **1**, **3** and **5** using the mentioned method afforded the products **2**, **4** and **6** in good yields (76–88%).

The esters **7b–l** were synthesized according to the pervious work using carboxylic acids and alkyl halides in the presence of DBU (1,8-diazabicyclo[5,4,0]undec-7-ene) in benzene.[24]

3.2. Molecular modeling, docking and SAR study

3.2.1. Multiple alignment

Conserved amino acids were identified through multiple alignment in clustalX 1.81.[25] Sequences of lipoxygenase (LO) family were selected from blasted sequences via ExPASY proteomics server.[26] Multiple alignment process was then carried out on the selected sequences (protein weight matrix: BLOSUM series, opening gap penalty = 10).

3.2.2. Structure optimization

Structures **7a–l** were simulated in CHEM3D professional; Cambridge software; using MM2 method (RMS gradient = 0.05 kcal/mol).[27] Output files were minimized under semi-empirical AM1 method in the second optimization (convergence limit = 0.01; iteration limit = 50; RMS gradient = 0.05 kcal/mol; Fletcher-Reeves optimizer algorithm) in HYPERCHEM7.5.[28,29]

Crystal structure of soybean lipoxygenase-3 (arachidonate 15-lipoxygenase) complex with 13(*S*)-hydroproxy-9(*Z*)-2,11(*E*)-octadecadienoic acid and rabbit 15-lipoxygensae (type a) complex with (*E*)-3-(2-(oct-1-ynyl)phenyl)acrylic acid was retrieved from RCSB Protein Data Bank (PDB entry: 1IK3 and 2P0 M, respectively).

In this study, Van der Waals molecular volume (MV) was measured by QSAR properties tool in HYPERCHEM7.5.[28] The lipophilicity of amino acids was taken from ExPASy[26] (ProtScale) by applying Hphob (Kyte and Doolittle hydropathicity).

3.2.3. Molecular docking

Automated docking simulation was implemented to dock **7a–l** into the active site of SLO with AUTODOCKTOOLS version 1.4[30] using Lamarckian genetic algorithm.[31] This method has been previously

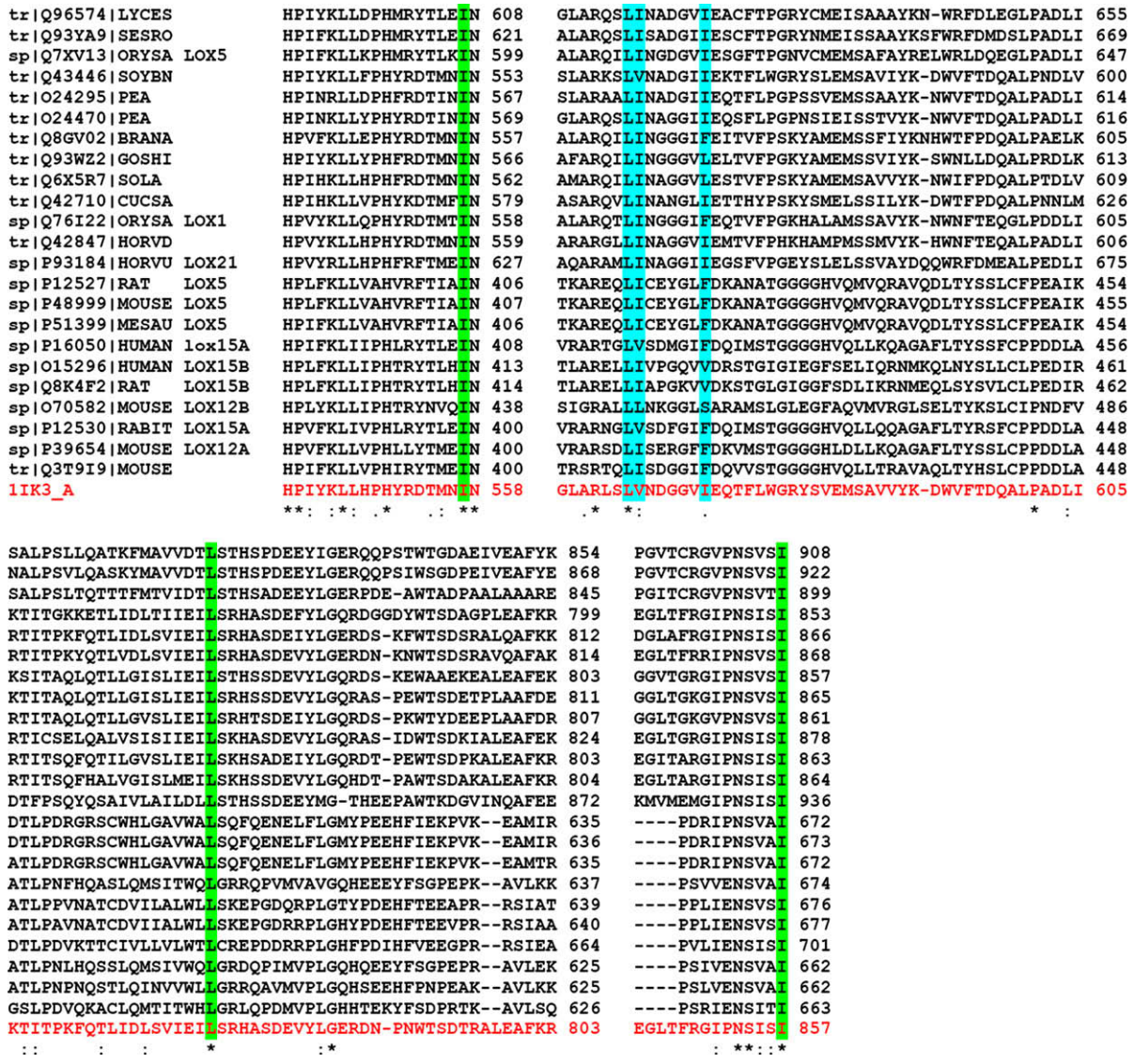

Figure 3. Multiple alignment of SLO (1ik3_A). The conserved residues of two pockets A and B are highlighted in green and blue, respectively.

shown to produce bonding models similar to the experimentally observed models.[29,31,32] The torsion angles of the ligands were identified, hydrogens were added to the macromolecule, bond distances were edited and solvent parameters were added to the enzyme 3D structure. Partial atomic charges were then assigned to the macromolecule as well as ligands (Gasteiger for the ligands and Kollman for the protein).

The regions of interest of the enzyme were defined by considering Cartesian chart 19.9, 4.3 and 15.5 as the central of a grid size of 30, 30 and 40 points in *X*, Y and *Z-axes*. The docking parameter files were generated using Genetic Algorithm and Local Search Parameters (GALS) while number of generations was set to 100. Compounds **7a–l** were each docked into the active site of SLO enzyme and the simulations were composed of 100 docking runs, each of 50 cycles containing a maximum of 10,000 accepted and rejected steps. The simulated annealing procedure was started at high temperature (RT = 616 kcal/mol, where R is the gas constant and T is the steady state temperature) and was decreased by a fraction of 0.95 on each cycle[33] The 100 docked complexes were clustered with a root-mean-square deviation tolerance of 0.2 Å. Autodock generated 100 docked conformers of **7a–l** corresponding to the lowest-energy structures. After docking procedure in AD3, docking results were submitted to Weblab Viewerlite 4.0[34] and Swiss-PdbViewer 3.7 (spdbv)[35] for further evaluations. The results of docking processing (ΔG_b: estimated free energy of bonding, E_d: final docked energy and K_i: estimated inhibition constant) are outlined in Table 1.

3.2.4. Protein modeling

Three-dimensional models of the 15-HLOa and 15-HLOb sequences were constructed by homology modeling. BLAST sequence homology searches were performed in order to identify the template proteins. The rabbit 15-lipoxygensae (type a) complex with (*E*)-3-(2-(oct-1-ynyl)phenyl)acrylic acid (15-RLOa, PDB entry: 2P0 M) was chosen as the template for modeling the proteins. The identity of 15-HLOa and 15-HLOb with 15-RLOa is 77% and 37%, respectively. Model building was performed in the program MODELLER9V1 using model-ligand algorithm.[1] Several models at various refinement levels were generated and finally the refined structures involved (*E*)-3-(2-(oct-1-ynyl)phenyl)acrylic acid in the active site pocket, were minimized under molecular mechanic AMBER method (RMS gradient = 1) in HYPERCHEM7.5.[28] All

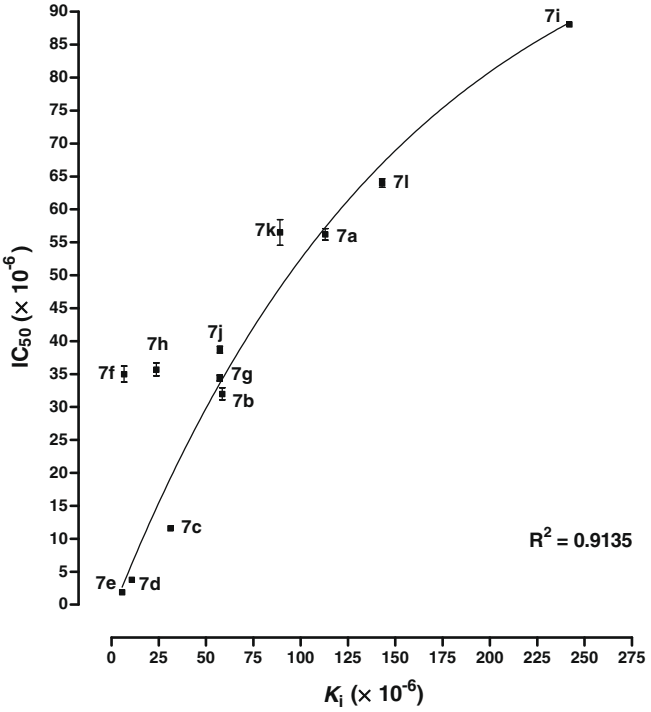

Figure 4. Diagram of IC_{50} value versus K_i for compounds **7a–l**.

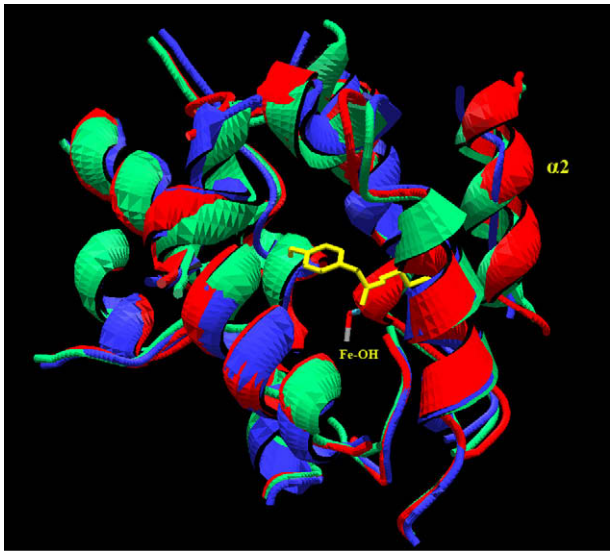

Figure 5. Comparison of three 15-LO 3D structures (in ribbon view). C-α of SLO, modeled 15-HLOa and b are superposed and colored in green, blue and red, respectively. The active site pockets were mapped by inserting the consensus structure of **7e**.

models were validated using the program ERRAT at UCLA.[36] The best model had an ERRAT score of 87% and 83% for 15-HLOa and 15-HLOb, respectively.

3.3. 15-LO inhibitory assessment

15-Lipoxygenase activity was measured in borate buffer solutions (0.1 M, pH 9) for soybean enzyme and Tris–HCl (50 mM, pH 7.2) for human type enzyme using the method described in literature,[37,38] by measuring the absorbance at 234 nm for 60–120 s after addition of the enzyme and linoleic acid (final concentration: 134 μM) as substrate at 20 ± 1 °C. The final enzyme concentration was 10 μg/mL. Synthesized substances were added in DMSO solutions (final DMSO concentration 1%); whereas DMSO was added in control experiments with no inhibitor. The mixture of each inhibitors and linoleic acid was set as blank sample in testing step. At least six control test tubes and three tubes for each inhibitor solution were measured. To ensure constant enzyme activity throughout the experiment, the enzyme solution was kept in ice, and controls were measured at regular intervals. Calculation of enzyme activity was carried out as previously described[38] and IC_{50} values were determined by linear interpolation between the points around 50% activity (Table 1).

4. Experimental

4.1. Instruments

The ^{1}H NMR (100 MHz) spectra were recorded on a Bruker AC 100 spectrometer. Elemental analysis was obtained on a Thermo Finnigan Flash EA microanalyzer. The IR spectra were obtained on a 4300 Shimadzu Spectrometer. All measurements of lipoxygenase activities were carried out using an Agilent 8453 spectrophotometer. The soybean 15-lipoxygenase and other chemicals were purchased from Sigma, Aldrich and Merck Co., respectively. Human recombinant 15-lipoxygenase a and b (I and II, expressed in *E. coli*) was prepared from Cyman Chemical Co.

4.2. General procedure for preparation of compounds 2, 4 and 6

To a 0 °C suspension consisting of Mg (1.92 g, 80 mmol), $TiCl_4$ (3.79 g, 2.1 mL, 20 mmol), and CH_2Cl_2 (40 mL) was added over a 20 min period a solution of the corresponding ketone (10 mmol) in CH_2Cl_2 (30 mL) and THF (20 mL). After being stirred for 30 min at 0 °C, the resulting green–black mixture was stirred for an additional 20 min at room temperature. The reaction mixture was recooled to 0 °C. Saturated potassium carbonate solution (100 mL) was added and the mixture was diluted with ether (200 mL). The organic layer was separated, dried, evaporated, and purified by vacuum distillation.

4.2.1. 1-Methoxy-4-(2-methylallyl)benzene 2

Colorless oil; yield 88%; bp 76–78 °C/3 mm; ^{1}H NMR ($CDCl_3$): δ 1.68 (s, 3H, –C*H*$_3$), 3.27 (s, 2H, –C*H*$_2$–), 3.80 (s, 3H, –OC*H*$_3$), 4.81 (d, J = 1.2 Hz, 1H, *H*C═C), 4.84 (d, J = 1.2 Hz, 1H, *H*C═C), 6.84 (d, J = 8.6 Hz, 2H, H-3, H-5), 7.12 (d, J = 8.6 Hz, 2H, H-2, H-6); IR cm^{-1}: 1608 (C═C); Found: C, 81.21; H, 8.83. $C_{11}H_{14}O$ requires: C, 81.44; H, 8.70.

4.2.2. 1-Methoxy-4-(2-ethylallyl)benzene 4

Colorless oil; yield 83%; bp 83–84 °C/3 mm; ^{1}H NMR ($CDCl_3$): δ 0.90 (t, 3H, J = 7.3 Hz, –C*H*$_3$), 1.74 (q, 2H, J = 7.3 Hz, –C*H*$_2$–), 3.27 (s, 2H, –C*H*$_2$–), 3.80 (s, 3H, –OC*H*$_3$), 4.81 (d, J = 1.2 Hz, 1H, *H*C═C), 4.84 (d, J = 1.2 Hz, 1H, *H*C═C), 6.84 (d, J = 8.6 Hz, 2H, H-3, H-5), 7.12 (d, J = 8.6 Hz, 2H, H-2, H-6); IR cm^{-1}: 1610 (C═C); Found: C, 82.01; H, 9.13. $C_{12}H_{16}O$ requires: C, 81.77; H, 9.15.

4.2.3. 1,2,3,4-Tetrahydro-6-methoxy-2-methylenenaphthalen 6

Colorless oil; yield 76%; bp 120–123 °C/3 mm; ^{1}H NMR ($CDCl_3$): δ 2.45 (t, J = 6.5 Hz, 2H, (C*H*$_2$)$_2$C═C), 2.84 (t, J = 6.3 Hz, 2H, (C*H*$_2$)$_2$C═C), 3.46 (s, 2H, –C*H*$_2$–), 3.77 (s, 3H, –OC*H*$_3$), 4.81 (d, J = 1.2 Hz, 1H, *H*C═C), 4.84 (d, J = 1.2 Hz, 1H, *H*C═C), 6.65 (s, 1H, H-5), 6.69 (d, J = 8.6 Hz, 1H, H-7), 6.99 (d, J = 8.6 Hz, 1H, H-8); IR cm^{-1}: 1612 (C═C); Found: C, 82.21; H, 8.08. $C_{12}H_{14}O$ requires: C, 82.72; H, 8.01.

Table 2
The Kyte and Doolittle hydropathicity (Hphob) and Van der Waals molecular volume (MV) of superposed amino acids within 7 Å around the LA into SLO X-ray view

SLO	HLOa	HLOb	SLO	HLOa	HLOb
[Leu^{273} Thr^{274} Leu^{277}]	[Ile^{173} Asp^{174}]	[Gln^{119} Glu^{120} Ala^{123}]	Leu^{565} Val^{566} Ile^{572}	Leu^{408} Val^{409} Phe^{415}	Leu^{420} Ile^{421} Val^{427}
Val^{372}	Ala^{237}	Arg^{221}	Phe^{576}	Met^{419}	Thr^{431}
Asn^{373}	Asn^{238}	Thr^{222}	His^{709}	His^{541}	His^{553}
Val^{506}	Arg^{349}	Arg^{361}	Asn^{713}	His^{545}	Ser^{557}
Asp^{509}	Asp^{352}	Glu^{364}	Glu^{716}	Glu^{548}	Gln^{560}
Ser^{510}	Phe^{353}	Phe^{365}	Gly^{720}	Phe^{552}	Cys^{564}
His^{513}	His^{356}	His^{368}	Arg^{726}	Ala^{558}	Leu^{570}
Gln^{514}	Glu^{357}	Glu^{369}	Pro^{727}	Pro^{559}	Pro^{571}
Leu^{515}	Leu^{358}	Ala^{370}	Thr^{728}	Cys^{560}	Pro^{572}
His^{518}	His^{361}	His^{373}	Asp^{766}	Gln^{590}	Val^{603}
Trp^{519}	Leu^{362}	Leu^{374}	Val^{769}	Ile^{593}	Ala^{606}
His^{523}	His^{366}	His^{378}	Ile^{770}	Val^{594}	Leu^{607}
Ile^{557}	Ile^{400}	Ile^{412}	Ile^{772}	Gln^{596}	Leu^{609}
Leu^{560}	Arg^{403}	Leu^{415}	Leu^{773}	Leu^{597}	Leu^{610}
Ala^{561}	Ala^{404}	Ala^{416}	Ile^{857}	Ile^{663}	Ile^{676}

AA	Hphob	MV	AA	Hphob	MV	AA	Hphob	MV	AA	Hphob	MV
Ala	1.30	71.21	Arg	−4.50	151.63	Asn	−3.50	99.58	Asp	−3.50	92.73
Cys	2.50	93.87	Gln	−3.50	116.24	Glu	−3.50	109.14	Gly	−0.40	54.52
His	−3.20	126.23	Ile	4.50	119.85	Leu	3.80	120.27	Lys	−3.90	134.37
Met	1.90	157.91	Phe	2.80	144.37	Pro	−1.60	85.01	Ser	−0.80	78.04
Thr	−0.70	94.65	Trp	−0.90	170.47	Tyr	−1.30	149.97	Val	4.20	103.62

AA = Amino acid.

4.3. General procedure for preparation of esters 7b–l

A mixture of corresponding alkyl bromide (45 mmol for primary and 54 mmol for secondary alkyl bromide), 4-methoxyphenylacetic acid (4.98 g, 30 mmol), DBU (4.56 g, 30 mmol) and 60 mL of benzene was refluxed for 3–6 h regarding the primary or secondary type of alkyl bromide. The reaction mixture was then washed with water, dried over anhydrous magnesium sulfate and distilled. For ester **7b**, ethyl iodide was used and the reaction time reduced to 2 h at room temperature.

Ester **7j** was synthesized by adding gradually 4-methoxyphenyl acetyl chloride (1.84 g, 10 mmol) to a mixture of *tert*-butyl alcohol (0.72 g, 9.7 mmol), triethylamine (1.2 g, 10 mmol) and dichloromethane (1.5 mL) follow refluxing for 1 h. Isolation and purification of desired product was down according to the mentioned procedure.

4.3.1. Ethyl 2-(4-methoxyphenyl)acetate 7b

Colorless oil; yield 86%; bp 103–105 °C/3 mm; ^{1}H NMR ($CDCl_3$): δ 1.23 (t, J = 7.1 Hz, 3H, –CH_3), 3.52 (s, 2H, –CH_2–), 3.77 (s, 3H, –OCH_3), 4.13 (q, J = 7.0 Hz, 1H, –OCH_2–), 6.84 (d, J = 8.6 Hz, 2H, H-3, H-5), 7.19 (d, J = 8.6 Hz, 2H, H-2, H-6); IR cm^{-1}: 1733 (C=O); Found: C, 68.09; H, 7.25. $C_{11}H_{14}O_3$ requires: C, 68.02; H, 7.27.

4.3.2. Propyl 2-(4-methoxyphenyl)acetate 7c

Colorless oil; yield 82%; bp 122–124 °C/2 mm; ^{1}H NMR ($CDCl_3$): δ 0.90 (t, J = 7.2 Hz, 3H, –CH_3), 1.45–1.85 (m, 2H, –OCH$_2$CH_2CH$_3$), 3.54 (s, 2H, –CH_2–), 3.78 (s, 3H, –OCH_3), 4.03 (t, J = 6.8 Hz, 2H, –OCH_2CH$_2$CH$_3$), 6.84 (d, J = 8.6 Hz, 2H, H-3, H-5), 7.19 (d, J = 8.6 Hz, 2H, H-2, H-6); IR cm^{-1}: 1735 (C=O); Found: C, 69.29; H, 7.80. $C_{12}H_{16}O_3$ requires: C, 69.21; H, 7.74.

4.3.3. Butyl 2-(4-methoxyphenyl)acetate 7d

Colorless oil; yield 80%; bp 136–138 °C/3 mm; ^{1}H NMR ($CDCl_3$): δ 0.92 (t, J = 6.3 Hz, 3H, –CH_3), 1.18–1.85 (m, 4H, –OCH$_2$(CH_2)$_2$CH$_3$), 3.58 (s, 2H, –CH_2–), 3.93 (s, 3H, –OCH_3), 4.07 (t, J = 6.4 Hz, 2H, –OCH_2(CH$_2$)$_2$CH$_3$), 6.85 (d, J = 8.7 Hz, 2H, H-3, H-5), 7.21 (d, J = 8.7 Hz, 2H, H-2, H-6); IR cm^{-1}: 1735 (C=O); Found: C, 70.21; H, 8.06. $C_{13}H_{18}O_3$ requires: C, 70.24; H, 8.16.

4.3.4. Pentyl 2-(4-methoxyphenyl)acetate 7e

Colorless oil; yield 70%; bp 148–149 °C/3 mm; ^{1}H NMR ($CDCl_3$): δ 0.91 (t, J = 6.3 Hz, 3H, –CH_3), 1.20–1.80 (m, 4H, –OCH$_2$(CH_2)$_2$CH$_3$), 3.56 (s, 2H, –CH_2–), 3.80 (s, 3H, –OCH_3), 4.08 (t, J = 6.4 Hz, 2H, –OCH_2(CH$_2$)$_2$CH$_3$), 6.87 (d, J = J = 8.7 Hz, 2H, H-3, H-5), 7.18 (d, J = 8.7 Hz, 2H, H-2, H-6); IR cm^{-1}: 1735 (C=O); Found: C, 71.27; H, 8.61. $C_{14}H_{20}O_3$ requires: C, 71.15; H, 8.53.

4.3.5. Hexyl 2-(4-methoxyphenyl)acetate 7f

Colorless oil; yield 71%; bp 160–161 °C/3 mm; ^{1}H NMR ($CDCl_3$): δ 0.88 (t, J = 6.3 Hz, 3H, –CH_3), 1.13–1.81 (m, 8H, –OCH$_2$(CH_2)$_4$CH$_3$), 3.54 (s, 2H, –CH_2–), 3.79 (s, 3H, –OCH_3), 4.10 (t , J = 6.4 Hz, 2H, –OCH_2(CH$_2$)$_2$CH$_3$), 6.86 (d, J = 8.6 Hz, 2H, H-3, H-5), 7.22 (d, J = 8.6 Hz, 2H, H-2, H-6); IR cm^{-1}: 1734 (C=O); Found: C, 72.31; H, 8.92. $C_{15}H_{22}O_3$ requires: C, 71.97; H, 8.86.

4.3.6. Isopropyl 2-(4-methoxyphenyl)acetate 7g

Colorless oil; yield 81%; bp 120–122 °C/3 mm; ^{1}H NMR ($CDCl_3$): δ 1.20 (d, J = 6.2 Hz, 6H, (H_3C)$_2$CHO–), 3.49 (s, 2H, –CH_2–), 3.77 (s, 3H, –OCH_3), 4.78–5.15 (m, 1H, –OCH(CH$_3$)$_2$), 6.83 (d, J = 8.6 Hz, 2H, H-3, H-5), 7.18 (d, J = 8.6 Hz, 2H, H-2, H-6); IR cm^{-1}: 1735 (C=O); Found: C, 69.18; H, 7.70. $C_{12}H_{16}O_3$ requires: C, 69.21; H, 7.74.

4.3.7. *sec*-Butyl 2-(4-methoxyphenyl)acetate 7h

Colorless oil; yield 83%; bp 127–128 °C/3 mm; ^{1}H NMR ($CDCl_3$): δ 0.86 (t, J = 7.1 Hz, 3H, –OCH(CH$_3$)CH$_2$CH_3), 1.20 (d, J = 6.06 Hz, 3H, –OCH(CH_3)CH$_2$CH$_3$), 1.41–1.75 (m, 2H, –OCH(CH$_3$)CH_2CH$_3$), 3.54 (s, 2H, –CH_2–), 3.79 (s, 3H, –OCH_3), 4.68–5.03 (m, 1H, –OCH(CH$_3$)CH$_2$CH$_3$), 6.86 (d, J = 8.6 Hz, 2H, H-3, H-5), 7.22 (d, J = 8.6 Hz, 2H, H-2, H-6); IR cm^{-1}: 1735 (OC=O); Found: C, 70.39; H, 8.13. $C_{13}H_{18}O_3$ requires: C, 70.24; H, 8.16.

4.3.8. Isobutyl 2-(4-methoxyphenyl)acetate 7i

Colorless oil; yield 79%; bp 129–131 °C/3 mm; ^{1}H NMR ($CDCl_3$): δ 0.87 (d, J = 6.6 Hz, 6H, (H_3C)$_2$CHCH$_2$O–), 1.71–2.14 (m, 1H, –OCH$_2$CH(CH$_3$)$_2$), 3.54 (s, 2H, –CH_2–), 3.76 (s, 3H, –OCH_3), 3.85 (d, J = 6.6 Hz, 2H, –OCH_2CH(CH$_3$)$_2$), 6.83 (d, J = 8.6 Hz, 2H, H-3,

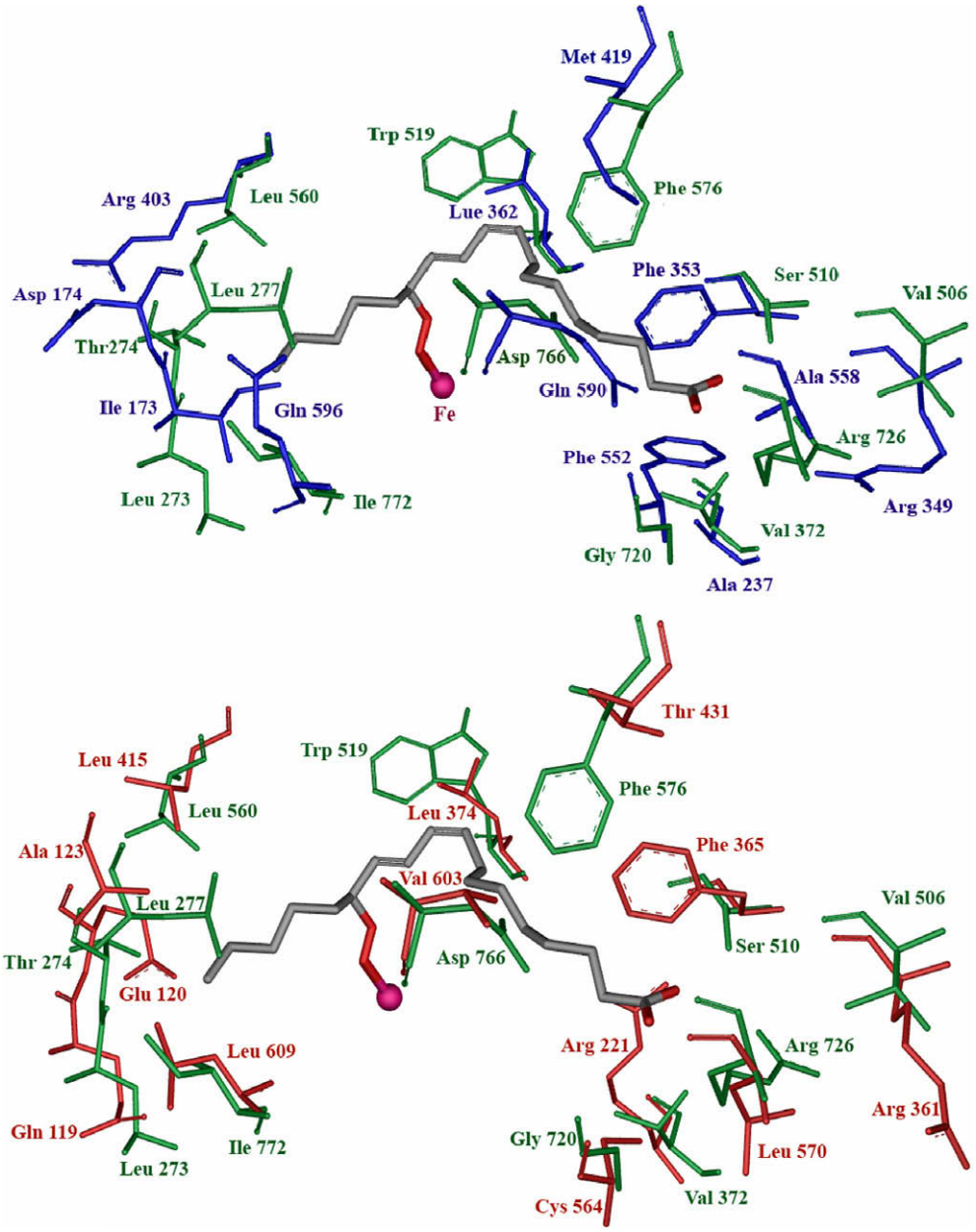

Figure 6. Stick view of LA bond to Fe and C-α superposed amino acids of 15-HLOa (blue), 15-HLOb (red) and SLO (green) which have high differences in molecular volume and lipophilicity.

H-5), 7.20 (d, J = 8.6 Hz, 2H, H-2, H-6); IR cm^{-1}: 1735 (C═O); Found: C, 70.17; H, 8.19. $C_{13}H_{18}O_3$ requires: C, 70.24; H, 8.16.

4.3.9. *tert*-Butyl 2-(4-methoxyphenyl)acetate 7j

Colorless oil; yield 48%; bp 89–92 °C/3 mm; ^{1}H NMR ($CDCl_3$): δ 1.44 (s, 9H, $(H_3C)_3CO$–), 3.46 (s, 2H, –CH_2–), 3.78 (s, 3H, –OCH_3), 6.85 (d, J = 8.6 Hz, 2H, H-3, H-5), 7.22 (d, J = 8.6 Hz, 2H, H-2, H-6); IR cm^{-1}: 1738 (OC═O); Found: C, 70.33; H, 8.10. $C_{13}H_{18}O_3$ requires: C, 70.24; H, 8.16.

4.3.10. Cyclopentyl 2-(4-methoxyphenyl)acetate 7k

Colorless oil; yield 77%; bp 145–147 °C/3 mm; ^{1}H NMR ($CDCl_3$): δ *1.48–1.98* (m, 8H, –CH_2– (cyclopentyl)), 3.50 (s, 2H, –CH_2–), 3.78 (s, 3H, –OCH_3), 5.04–5.28 (m, 1H, –CH– (cyclopentyl)), 6.85 (d, J = 8.7 Hz, 2H, H-3, H-5), 7.19 (d, J = 8.7 Hz, 2H, H-2, H-6); IR cm^{-1}: 1735 (C═O); Found: C, 71.61; H, 7.81. $C_{14}H_{18}O_3$ requires: C, 71.77; H, 7.74.

4.3.11. Cyclohexyl 2-(4-methoxyphenyl)acetate 7l

Colorless oil; yield 74%; bp 155–156 °C/2 mm; ^{1}H NMR ($CDCl_3$): δ *1.18–2.00* (m, 10H, –CH_2– (cyclohexyl)), 3.54 (s, 2H, –CH_2–), 3.80 (s, 3H, –OCH_3), 4.61–4.93 (m, 1H, –CH– (cyclohexyl)), 6.86 (d, J = 8.6 Hz, 2H, H-3, H-5), 7.22 (d, J = 8.6 Hz, 2H, H-2, H-6); IR cm^{-1}: 1735 (C═O); Found: C, 72.31; H, 8.05. $C_{15}H_{20}O_3$ requires: C, 72.55; H, 8.12.

References and notes

1. Sadeghian, H.; Seyedi, S. M.; Saberi, M. R.; Arghiani, Z.; Riazi, M. *Bioorg. Med. Chem.* **2008**, *16*, 890.
2. Brash, A. R. *J. Biol. Chem.* **1999**, *274*, 23679.
3. Kuhn, H.; Thiele, B. *J. FEBS Lett.* **1999**, *449*, 7.
4. Larsen, J. S.; Acosta, E. P. *Ann. Pharmacother.* **1993**, *27*, 898.
5. Schewe, T. *Biol. Chem.* **2002**, *383*, 365.
6. Kelavkar, U.; Glasgow, W.; Eling, T. E. *Curr. Urol. Rep.* **2002**, *3*, 207.
7. Kelavkar, U. P.; Cohen, C.; Kamitani, H.; Eling, T. E.; Badr, K. F. *Carcinogenesis* **2000**, *21*, 1777.

8. Zhu, J.; Kilty, I.; Granger, H.; Gamble, E.; Qiu, Y. S.; Hattotuwa, K.; Elston, W.; Liu, W. L.; Liva, A.; Pauwels, R. A.; Kis, J. C.; De Rose, V.; Barnes, N.; Yeadon, M.; Jenkinson, S.; Jeffery, P. K. *Am. J. Respir. Cell Mol. Biol.* **2002**, *27*, 666.
9. Zhao, L.; Funk, C. D. *Trends Cardiovasc. Med.* **2004**, *14*, 191.
10. Cyrus, T.; Witztum, J. L.; Rader, D. J.; Tangirala, R.; Fazio, S.; Linton, M. F.; Funk, C. D. *J. Clin. Invest.* **1999**, 1597.
11. Harats, D.; Shaish, A.; George, J.; Mulkins, M.; Kurihara, H.; Levkovitz, H.; Sigal, E. *Arteriosler. Thromb. Vasc. Biol.* **2000**, *20*, 2100.
12. Sultana, C.; Shen, Y.; Rattan, V.; Kalra, V. J. *J. Cell. Phys.* **1996**, *167*, 467.
13. Setty, B. N.; Werner, M. H.; Annun, Y. A.; Stuart, M. *J. Blood* **1992**, *80*, 2765.
14. Zhao, L.; Funk, C. D. *Trends Cardiovasc. Med.* **2004**, *14*, 191.
15. Chanez, P.; Bonnans, C.; Chavis, C.; Vachier, I. *Am. J. Respir. Cell Mol. Biol.* **2002**, *27*, 655.
16. Shappell, S. B.; Boeglin, W. E.; Olson, S. J.; Kasper, S.; Brash, A. R. *Am. J. Pathol.* **1999**, *155*, 235.
17. Hsi, L. C.; Wilson, L. C.; Eling, T. E. *J. Biol. Chem.* **2002**, *277*, 40549.
18. Charlier, C.; Michaux, C. *Eur. J. Med. Chem.* **2003**, *38*, 645.
19. Bakavoli, M.; Sadeghian, H.; Tabatabaei, Z.; Rezaei, E.; Rahimizadeh, M.; Nikpour, M. *J. Mol. Mod.* **2008**, *14*, 471.
20. Skrzypczak-Jankun, E.; Bross, R.; Carroll, R. T.; Dunham, W. R.; Funk, M. O., Jr. *J. Am. Chem. Soc.* **2001**, *123*, 10814.
21. Knapp, M. J.; Seebeck, F. P.; Klinman, J. P. *J. Am. Chem. Soc.* **2001**, *123*, 2931.
22. Choi, J.; Chon, J. K.; Kim, S.; Shin, W. *Proteins* **2007**, *70*, 1023.
23. Yan, T. H.; Tsai, C. C.; Chein, C. T.; Cho, C. C.; Huang, P. C. *J. Org. Lett.* **2004**, *6*, 4961.
24. Ono, N.; Yamada, T.; Saito, T.; Tanaka, K.; Kaji, A. *Bull. Chem. Soc. Jpn.* **1978**, *51*, 2401.
25. Thompson, J. D.; Gibson, T. J.; Plewniak, F.; Jeanmougin, F.; Higgins, D. G. *Nucleic Acids Res.* **1997**, *24*, 4876.
26. http://us.expasy.org/.
27. ChemDraw® Ultra, *Chemical Structure Drawing Standard*, CambridgeSoft Corporation, 100 Cambridge Park Drive, Cambridge, MA 02140 USA, http://www.cambrigesoft.com.
28. HyperChem® Release 7, Hypercube Inc., http://www.hyper.com/.
29. Bakavoli, M.; Nikpour, M.; Rahimizadeh, M.; Saberi, M. R.; Sadeghian, H. *Bioorg. Med. Chem.* **2007**, *15*, 2120.
30. Auto Dock Tools (ADT), *the Scripps Research Institute*, 10550 North Torrey Pines Road, La Jolla, CA 92037-1000, USA; (http://www.scripps.edu/pub/olson-web/doc/autodock/): Python, M. F. S. *J. Mol. Graph. Mod.* **1999**, *17*, 57.
31. Morris, G. M.; Goodsell, D. S.; Halliday, R. S.; Huey, R.; Hart, W. E.; Belew, R. K.; Olson, A. J. *J. Comput. Chem.* **1998**, *19*, 1639.
32. Sippl, W. *J. Comput. Aided Mol. Des.* **2000**, *14*, 559.
33. Dym, O.; Xenarios, I.; Ke, H.; Colicelli, J. *Mol. Pharmacol.* **2002**, *61*, 20.
34. http://sunfire.vbi.vt.edu/gcg/seqweb-guides/WebLab_Viewer.html.
35. Swiss-pdbViewer 3.6, *Glaxo Wellcome Experimental Research*, http://www.expasy.org/spdbv/.
36. http://nihserver.mbi.ucla.edu/savs/.
37. Malterud, K. E.; Rydland, K. M. *J. Agric. Food Chem.* **2000**, *48*, 5576.
38. Malterud, K. E.; Farbrot, T. L.; Huse, A. E.; Sund, R. B. *Pharmacology* **1993**, *47*, 77 (Suppl 1).